A Computational Model for the Simulation of Millimeter-Wave Propagation Through the Clear Atmosphere

Jerry D. Hopponen
Hans J. Liebe

TABLE OF CONTENTS

LIST OF FIGURES

A COMPUTATIONAL MODEL FOR THE SIMULATION OF
MILLIMETER-WAVE PROPAGATION THROUGH THE CLEAR ATMOSPHERE

Jerry D. Hopponen and Hans J. Liebe*

Prediction of propagation effects (i.e., path attenuation, phase delay, ray bending, and medium noise) over the 1 to 300 GHz frequency range through the clear, nonturbulent atmosphere is accomplished by combining a spectroscopic data base with a computer program for two-dimensional ray tracing. Interactions between the physical environment and electromagnetic radiation are expressed by a complex refractivity N. The quantity N is a function of frequency, pressure, humidity, and temperature. Spectroscopic data supporting N consist of more than 450 coefficients describing local O_2 and H_2O absorption lines complemented by continuum spectra for dry air and water vapor. Height profiles (up to 80 km) of N-spectra are the basis for calculating propagation effects along a radio path (ground-to-ground, ground-to-aircraft, and ground-to-satellite). The computer model assumes a symmetric, spherically stratified atmosphere without horizontal N gradients. Evaluation of path integrals for radio range, cumulative attenuation, and noise temperature is accomplished in a rapid manner. Various simulated propagation aspects and details of the treatment of the noise integrals are given.

Key words: clear atmosphere; millimeter-wave propagation; path attenuation and delay; radiances; radio path modeling; ray bending

1.   INTRODUCTION

Performance assessment of millimeter wave systems that transmit or receive through the Earth's atmosphere is facilitated by considering a propagation module (climatological influences) and a nonpropagation module (hardware, software, etc.). For reliable system design as well as for adaptive compensations of atmospheric propagation effects, it is imperative that a model for simulating atmospheric transfer characteristics be available. The formulation presented here combines a broadband model of the complex refractive index of clear air with a ray tracing program in order to calculate radio path properties over the extended EHF (1 to 300 GHz) frequency range.

---
*Jerry D. Hopponen is with Lockheed Missiles and Space Company, Sunnyvale, CA 94086 (formerly with NTIA/ITS, Boulder, CO); Hans J. Liebe is with the Institute for Telecommunication Sciences, National Telecommunications and Information Administration, U.S. Department of Commerce, 325 Broadway, Boulder, CO 80303-3328.

The clear, nonturbulent air mass up to an altitude of 80 km acts as a unique filter of the EHF band with attenuation, delay, and noise characteristics not found at frequencies below 20 GHz. Absorption of radio waves by molecular oxygen and water vapor results in frequency-dependent attenuation, delay, and atmospheric emission; all of which, in return, offer remote-sensing opportunities on the atmospheric state. Propagation effects depend on the climatology assumed for the Earth-to-space path and may show considerable diurnal and seasonal variation. Therefore, although standard reference values may be available for the phenomena of interest, the careful assessment of propagation effects requires a computer model capable of making accurate predictions using any set of meteorological data.

The interaction of propagating radio waves with the atmosphere is described by a complex refractivity, N. In the EHF band, the frequency dependent components of N are primarily due to the absorption spectra of molecular oxygen and water vapor. Theoretical (Rosenkranz, 1975; Smith, 1981) and experimental (Liebe et al., 1977; Liebe, 1983; and references in Liebe, 1985) efforts have produced analytical expressions that are used in conjunction with a spectroscopic data base for the calculation of N as a function of frequency and meteorological variables. Characteristics of EHF propagation are simulated by generating a profile of N from a height distribution of clear air data and employing the N-profile in a ray-tracing methodology. Some details of the physical models and algorithms incorporated in the complete simulation program are discussed in order to set up a computer program in optimum manner.

2. ATMOSPHERIC INTERACTION WITH RADIATION

The first step in a simulation of electromagnetic wave propagation through the first 80 km of the Earth's atmosphere is a specification of the state of the medium. For a clear, nonturbulent atmosphere it is sufficient to give height profiles of total pressure, P; ambient temperature, T; and absolute humidity, v. These quantities are described by data specified (as in reference atmospheres or radiosonde data) at discrete altitudes all expressed in standard SI units (T in degrees Kelvin, P in Pascals, v in grams per cubic meter, and height in meters). The requisite height transformation is given by List (1958) and the spectroscopic relations are found in Liebe (1985).

Properties of the propagation medium are expressed by a complex refractivity $N(P,T,v)$, which consists of three components

$$N = N_0 + D(f) + j N''(f) \qquad \text{ppm} \qquad (1)$$

where N_0 is the frequency-independent refractivity, and $D(f)$ and $N''(f)$ are frequency dependent dispersion and absorption terms arising from spectra exhibited by molecular oxygen and water vapor. The N-formulation is founded on up-to-date theoretical results, incorporates empirical correction terms, and is amenable to rapid execution on a main-frame computer.

Amplitude and phase responses of a plane radio wave generally are described by the propagation constant

$$\Gamma = -(\alpha/2) + j(20958f + \beta) \qquad \text{km}^{-1} \qquad (2)$$

where the specific power attenuation is

$$\alpha = 0.04192fN'' \qquad \text{Np/km}, \qquad (3a)$$

or, in units of decibel per km,

$$\alpha^* = 4.343\alpha \qquad \text{dB/km}; \qquad (3b)$$

the specific phase delay is

$$\beta = 0.02096f(N_0 + D) \qquad \text{radians/km} \qquad (4)$$

or, expressed in excess propagation delay,

$$t = (\beta/2\pi f)10^3 = 3.336(N_0 + D) \qquad \text{ps/km}; \qquad (5)$$

and the frequency, f is in units of gigahertz throughout. In a nonhomogeneous medium the variable N is integrated along a ray path, as discussed below. The complex refractivity, N, expressed in terms of measurable quantities, provides a macroscopic measure of the interaction between radiation and the absorbing molecules in moist air.

Prediction of the propagation effects along short horizontal paths may be accomplished via expressions (2) through (5). For the case of a curved path

refracted through a nonhomogeneous clear air mass (e.g., ground-to-satellite links, radar tracking, remote sensing), meteorological data profiles are used as input and then converted to corresponding profiles of N values for use in ray-tracing. It is advisable to store the N profiles on a computer disk file since ray tracing may be performed by several program executions. This approach affords some economy since it permits a separate main program for calculating N. Reducing the compiled size of the ray-tracing program embraces a philosophy of modular programming. It may happen that the atmospheric data are specified at altitudes that are relatively far apart, so that the derived N profile is of questionable value in ray tracing. Thus, interpolation on either the basic atmospheric data or on the N profile is required. Although working with the atmospheric data that, in a sense, count the absorber molecules of the path, there are advantages to having more height resolution directly in the N profile. Each addition to the atmospheric data profile requires three interpolations (for T, P, and v), which would be followed by a calculation of N. Such an approach is not only time consuming but also presumes that the ray-tracing program has the code to calculate N, contrary to the philosophy advocated earlier. Hence the necessary "closeness" of interpolated N values is determined by a convergence criterion in the adaptive numerical integration employed to evaluate the ray-tracing integrals. The number of altitudes needed is generally not known prior to program execution and depends on the given atmospheric data and the ray elevation angle.

The $N(h)$ structure over the first 3 km above surface level h_0 is critical for a successful prediction of refraction, affecting rays starting at h_0 under low (i.e., close to the horizontal) elevation angles, θ_0. Values of $N(h)$ that are missing in the input data are generated by interpolation. The interpolation for the real part of (1) neglects the dispersive term $D(f)$ (generally, $D < 0.01N_0$) and assumes an exponential decay of moist air refractivity with height in the form

$$N_0(h) = N_0^S(h_0)\exp[(h_0 - h)/h_s] \qquad \text{ppm.} \qquad (6a)$$

Surface refractivity N_0^S and scale height h_s are interrelated on the average via (Bean and Thayer, 1959)

$$h_s = 1/\ell n[1/[1-a] \qquad \text{km} \qquad (6b)$$

where

$$a = (7.32/N_0^S) \exp (0.00558N_0^S). \tag{6c}$$

Typically, h_S varies between 8.0 and 4.5 km when N_0^S changes from 280 to 450 ppm depending on surface humidity.

Linear interpolation for values of $N''(f)$ can be obtained at heights other than those of the original data profile. Ray-tracing calculations employing exponential interpolation yield values that differ at select frequencies that differ by less than 3 dB from those calculated with linear interpolation when the lower 20 km of atmospheric data are given at 1-km altitude intervals. However, it should be noted that when the same data set is reduced to model 5 km intervals, the disparity between the exponential and linear ray trace results grows to over 30 dB. Specific results are shown below in Table 1. The scale height for absorption varies with humidity distribution and frequency (e.g., between 11 and 1.9 km; see Liebe, 1985: TABLE 4).

By virtue of the interpolation methods for the real and imaginary parts of N, the spherically symmetric shells defined by the N profile can be subdivided into thinner shells, thus more nearly approximating a continuum of N values.

TABLE 1.

Interpolation Comparison for a Tangential Path ($\theta_0 = 0°$) Through the U.S. Standard Atmosphere (h = 0 to 80 km)

Frequency (GHz)	FULL DATA SET Δh = 1 km Attenuation A(dB)		SPARCE DATA SET Δh = 5 km Attenuation A(dB)	
	Linear	Exponential	Linear	Exponential
20	34.66	34.24	40.63	32.51
40	36.57	36.16	43.33	36.75
60	5749.7	5744.8	5803.1	5722.5
95	117.82	115.87	146.12	112.31
120	491.99	490.04	537.89	508.07

3. RAY PATH CHARACTERISTICS

3.1 Ray Tracing

Wave propagation over a radio path can be described when increments dx of the total path length ℓ, both in km, are assumed in the x direction. Simplifications are introduced that allow the application of numerical methods to three types of radio paths:

Path Type	Height Range h	Path Differential dx
horizontal		$\ell(\lesssim 50 \text{ km})$
vertical	h_0 to H	Δh
slant	h_0 to H	$(\Delta h)s$

The nonhomogeneous (vertical, slant) atmosphere is assumed to be spherically stratified in concentric layers of height intervals Δh, for which values of N can be specified.

Ray tracing is used for slant paths to determine the path extension factor defined by

$$s \equiv dx/dh \tag{7}$$

A "ray" may be regarded as a curve generated by successive normals to surfaces of constant phase of a propagating wave. For a nonhomogeneous atmosphere the phase velocity may vary from point to point, resulting in ray bending. A ray is assumed to start from the initial level h_0 with an elevation angle Θ_0 (measured from the horizontal) and proceeds through the atmosphere gaining the height interval $\Delta h = (h - h_0)$, while being subjected to refractive bending when $\Theta_0 < 90°$. During stable climatic conditions (i.e., a homogeneously stratified atmosphere), the path extension of a slant path down to about $\Theta_0 \geq 10°$ increases according to the secant law

$$s = (\sin \Theta_0)^{-1}. \tag{7a}$$

Zenith ($\theta_0 = 90°$) path behavior is said to be caused by "one" air mass.

The effects of both refraction and Earth's curvature determine for low-angle ($\theta_0 < 10°$) cases the path increments dx = (Δh)s, which are given by (Blake, 1968; Levine et al., 1973)

$$s = \left\{ 1 - \left[\left(\frac{10^6 + N_i}{10^6 + N_j} \right) \left(\frac{r_E + h_0}{r_E + h} \right) \cos \theta_0 \right]^2 \right\}^{-1/2} \tag{7b}$$

where $N_i = [N_0 + D(f)]_{h_0}$, $N_j = [N_0 + D(f)]_h$, and $r_E = 6357$ km is a standard (45° N) Earth radius. Equation (7b) is the spherical form of Snell's law and is strictly valid only when N is purely real. In the case at hand, values for N" are generally small compared with $N_{i,j} \approx N_0$. For very low elevation angles ($\theta_0 < 1°$) and values of h close to h_0, many fine steps of Δh are required and (7b) becomes numerically unstable. Approximations of the two terms containing $N_{i,j}$ and r_E are made by expanding both as power series and retaining terms of degree less than three (e.g., Blake, 1968). At this point, increments dx = (Δh)s become very sensitive to the height distributions of meteorological variables. For example, the tangential ($\theta_0 = 0°$) air mass through the U.S. Standard Atmosphere for dry air is 38 (35) times the zenith value, while for water vapor the tangential mass can vary betwen 70 (64) and 180 times the zenith case. Values in parenthesis give the air mass for $N_{i,j} = 0$ (that is, no refractive bending).

The path differential, dx, is used in the formulation of several integrals of interest. These integrals resist attempts at closed-form solution, owing to the height dependence in dx, and so must be evaluated by numerical methods. The adaptive numerical integration technique by Romberg is found to provide accurate and rapid results because of the way in which the input data is treated and also because of the nature of the integrands (Bauer, 1961). The Romberg method not only inserts additional points into a given height interval but also shifts to higher order schemes [e.g. trapezoidal rule (linear) to Simpson's rule (quadratic) and so on], thus accelerating the convergence of the algorithm. The adaptive feature is especially desirable since the number of points required to evaluate an integral across an atmospheric layer may vary as a function of layer "thickness" (i.e., the difference between the initial and terminal altitudes defining the layer) and the ray

in the lowest layer, so this layer is always subdivided into groups of 10 intervals of thicknesses: 0.5, 5.0, 50, . . . meters up from the surface to the first data point above the surface. These artificial layers are taken as the intervals of integration in the lowest part of the atmosphere.

3.2 Path Integrals

Radio range (real part of N)

$$R = \int_{h_0}^{H} [N_0(h) + D(f,h)]dx \qquad mm, \qquad (8)$$

particularly for low elevation angle cases, $\theta_0 < 5°$, is the first path integral to be evaluated by means of the ray-tracing routine. The dispersion term, D(f), adds a frequency-dependent component. Rays propagating at different frequencies will separate in space (and time). A radio range difference, ΔR, can be calculated by tracing rays with and without dispersion, D(f). The example in Figure 1 for a tangential path ($\theta_0 = 0$) reveals differences on the order $\Delta R \approx 0.3$ and -0.4 m at the frequencies 57 and 63 GHz, respectively. In theory, the two rays are separated by $\Delta h \approx 0.7$ m when exiting the atmosphere at H = 80 km; in practice, path attenuation A [see (9) below] on the order to 6000 dB disallows this case.

Digital transmission at high data rates (>0.2 Gbit/s), however, will be impaired at carrier frequencies where the atmosphere displays gradients dD/df across the channel bandwidth (>0.5 GHz). An example of pulse propagation (1 ns, trapezoidal shape) over a horizontal (homogeneous) path is shown in Figure 2. Shape distortion and pulse widening increase with the propagation distance ℓ. The time domain analysis (K. Allen and H. Liebe; private communication, 1985) has not been extended, so far, to address pulse transmission affected by R (and A).

Total attenuation along the ray path (imaginary part of N) is given by

$$A = \int_{h_0}^{H} \alpha^*(f,h)dx \qquad dB \qquad (9)$$

where $\alpha^*(h)$ is specific attenuation in dB/km (3b) as a function of height. Attenuation A, quantifies the amount of energy extracted from a plane wave for a one-way path through the atmosphere. Path attenuation may show considerable variations with season, as depicted by two examples in Figure 3

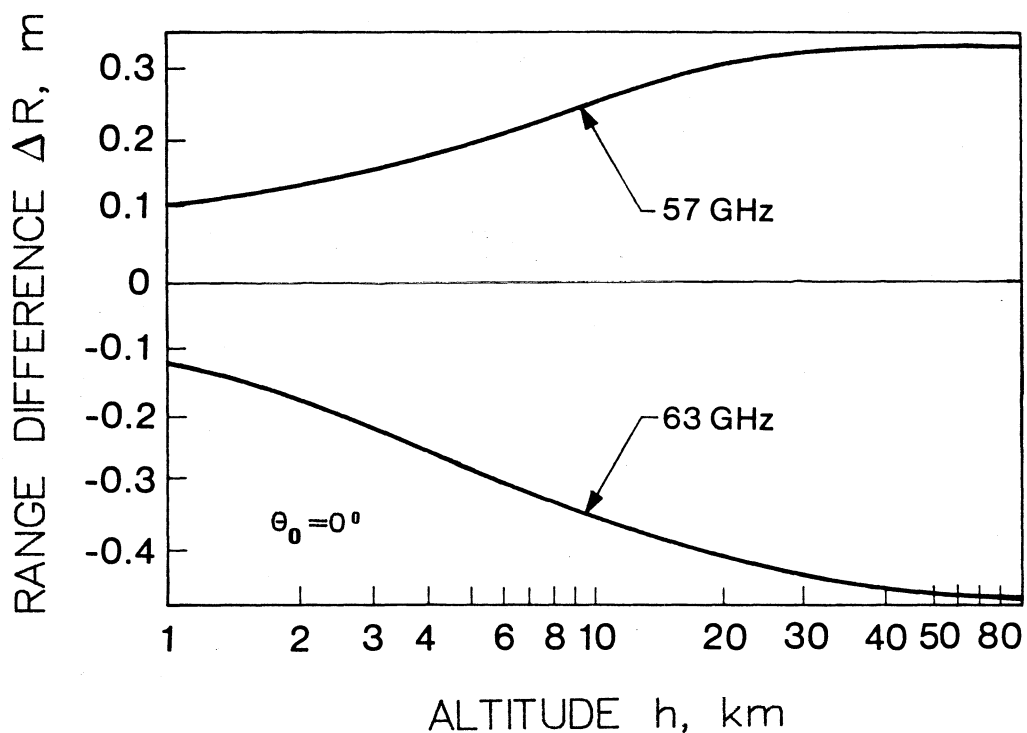# Tangential Path Dispersion
(Altitude Dependence)

Figure 1.   Radio range difference $\Delta R = R(N_0 + D) - R(N_0)$ due to atmospheric phase dispersion $D(f,h)$ for the frequency pair 57/63 GHz propagating at an elevation angle of 0° (tangential path) from sea level (h= 0 km) through a midlatitude summer atmosphere (Valley, 1976). The refractive radio range (H = 80 km) is $R(N_0)$ = 103.74 m; path attenuation A is on the order of 6000 dB at both frequencies (Liebe, 1983).

Pulse Distortion at Sea Level
(Path Length Dependence)
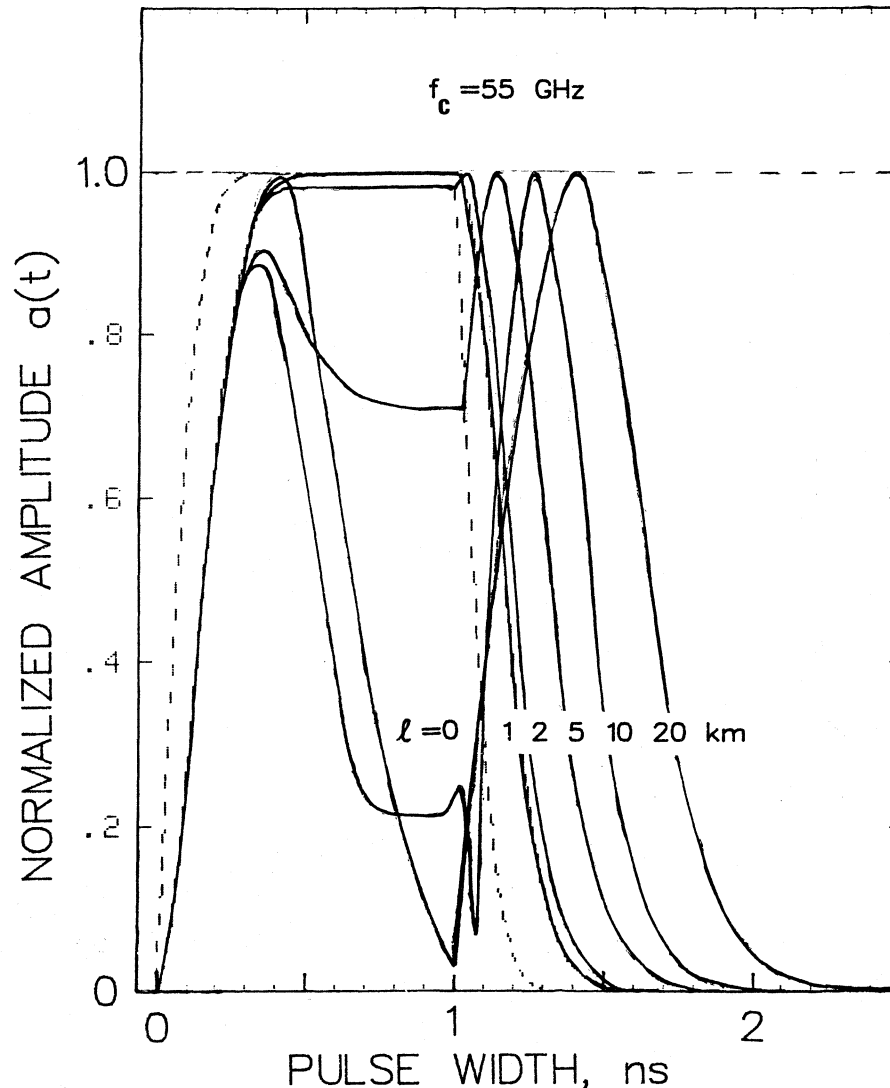
Figure 2. Normalized (a_{max} = 1) trapezoidal 1 ns-pulse at the carrier frequency f_c = 55 GHz propagating over a terrestrial path at sea level various distances, ℓ = 0 to 20 km.
The following meteorological conditions are assumed:

$$P = 1013 \text{ mb},$$
$$T = 15° C,$$
$$v = 11.5 \text{ g/m}^3 \text{ (90\%RH)},$$

leading at f_c = 55 GHz to the specific values
$$\alpha^* = 4.29 \text{ dB/km} \quad \text{and}$$
$$\beta = 0.916 \text{ radians/km}.$$

for a dry midlatitude winter atmosphere and a moist summer atmosphere. The fine structure resulting from the complex of O_2 lines centered around 60 GHz is not shown (see Liebe, 1983), but a crossover of the two curves is indicated, which results from the complicated temperature dependence in the spectral absorption expressions.

Radiance T_B indicates noise emission so that the atmosphere remains in thermal equilibrium and is expressed as equivalent blackbody temperature of radiation by the Rayleigh-Jeans approximation to Planck's law (Chandrasekar, 1950) in the form

$$T_B = \int T(x) \, \Phi(x) dx \qquad\qquad K, \qquad (10)$$

where

$$\Phi(x) = \alpha(x)\tau(x',x) \qquad\qquad km^{-1} \qquad (10a)$$

is a weighting function on $T(x)$, the local ambient temperature along the path; x' and x are two adjacent points; and τ is a transmittance to be defined below. Two cases can be made. In the first one, radiation upwelling from a starting height h_0 to the outer limit, H of the absorbing atmosphere (and possibly, continuing to a nadir-viewing satellite) leads to

$$T_B^{\uparrow} = \int_{h_0}^{H} \Phi_u T(x) dx \qquad\qquad K \qquad (11a)$$

(surface emission is not considered). Secondly, radiation downwelling to height h_0 (not necessarily the Earth's surface height) is described by

$$T_B^{\downarrow} = \int_{h_0}^{\infty} \Phi_d T(x) dx \qquad\qquad K \qquad (11b)$$

(cosmic background radiation of ≈ 2.7 K is not considered). The corresponding transmittances in Φ are defined by

$$\tau_u(h,H) \equiv exp[-\int_{h}^{H} \alpha(x)dx] \qquad (12a)$$

and

$$\tau_d(h_0,h) \equiv exp[-\int_{h_0}^{h} \alpha(x)dx]. \qquad (12b)$$

Zenith Path Attenuation
(Seasonal Extremes)

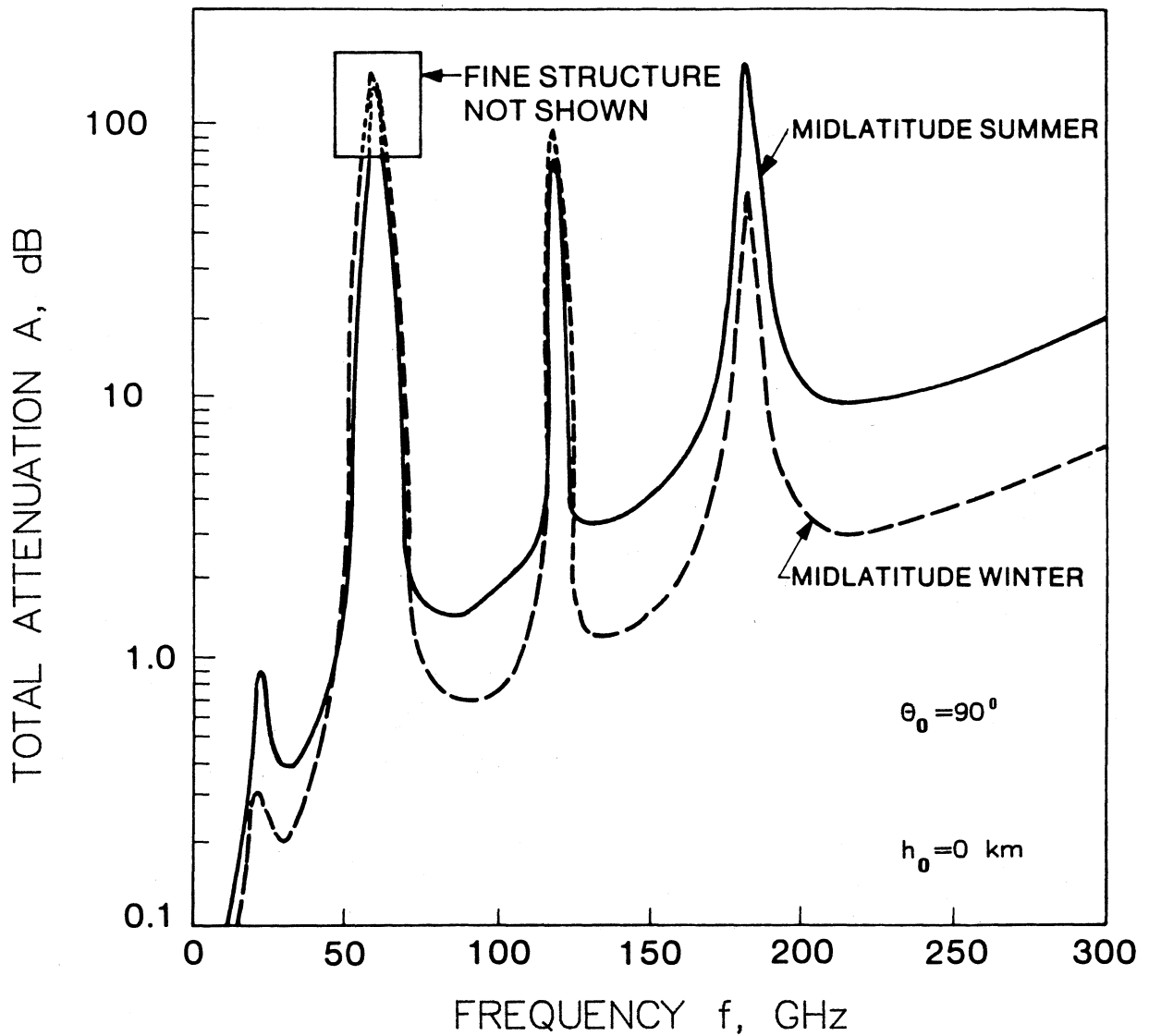Figure 3.   Seasonal variation of total, one-way attenuation A through a
dry winter and moist summer midlatitude atmospheres (Valley,
1976) along a vertical (zenith) Earth-to-space path.

They give the power loss from a point of height h to the reference heights, H or h_o. In both integrals, dx. is a differential of curved ray path (7b). The factor αT is, by the Raleigh-Jeans approximation, proportional to emission from a volume element of the absorbing air.

Figure 4 shows atmospheric noise due to vertical radiation upwelling to a satellite through two atmospheres representing extreme environmental conditions. The moist, tropical air mass generally yields higher noise temperatures than the dry, subarctic winter atmosphere. The actual behavior is dependent on the selected frequency as well as the physical conditions between 0 (h_o) and 80 (H) kilometers.

Figure 5 compares atmospheric contributions to upwelling and downwelling radiances through a vertical path in a midlatitude winter atmosphere. Except for regions of strong absorption, where the ground-based sensor receives radiation only from the immediate vicinity, the curves are nearly coincident across the EHF band.

Weighting functions Φ_u peaking at 58.82 GHz in the stratosphere are exhibited in Figure 6. The elevation angle θ_o at $h_o = 0$ varies the height from where maximum radiance originates between h = 18 ($\theta_o = 90°$) and h = 25 km ($\theta_o = 0°$). The radiance that can be detected under these conditions at H = 80 km (and beyond) is displayed in Figure 7. No radiance is received from the ground since the zenith attenuation $A(\theta_o = 90°)$ at this frequency is 140 dB. The temperature height profile of the particular model atmosphere accounts for the radiance structure as suggested by Figure 6. At this frequency there is less than 2 deg K variation, so the Earth appears from outer space as a nearly uniform noise source.

4. NOISE TEMPERATURE CALCULATION

The ray tracing methodology that is employed to compute the noise temperatures above begins with the specification of atmospheric data at heights

$$h_0 < h_1 < h_2 \cdot \cdot \cdot$$

The noise temperature integrals can then be written as

Zenith Path Radiance
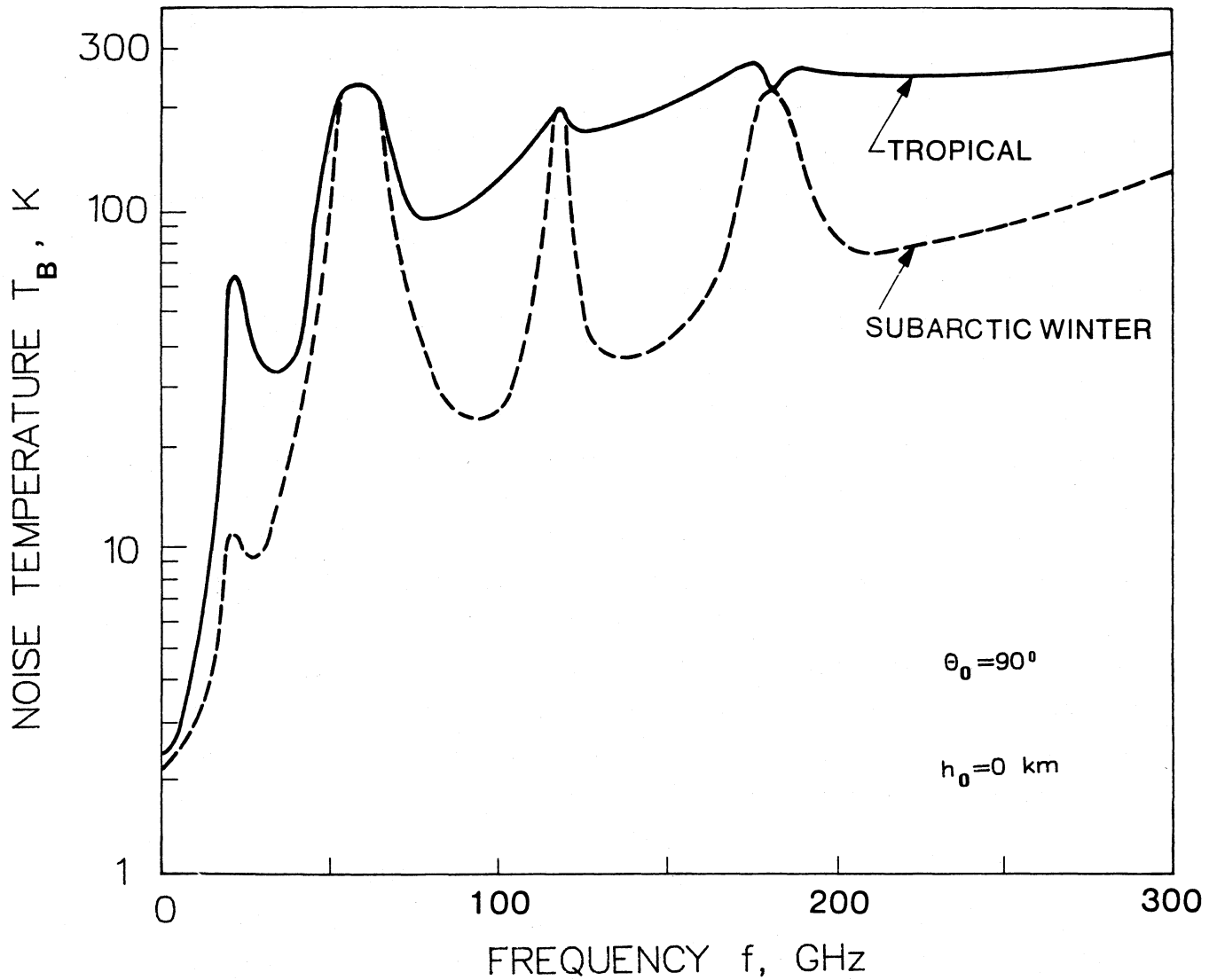# (Climatological Extremes)

Figure 4.   Upwelling atmospheric noise temperature (radiance) T_B from tropical and subarctic model atmospheres (Valley, 1976) representing environmental extreme conditions for a vertical Earth-to-space path.

Zenith Path Radiance
(Upwelling/Downwelling)
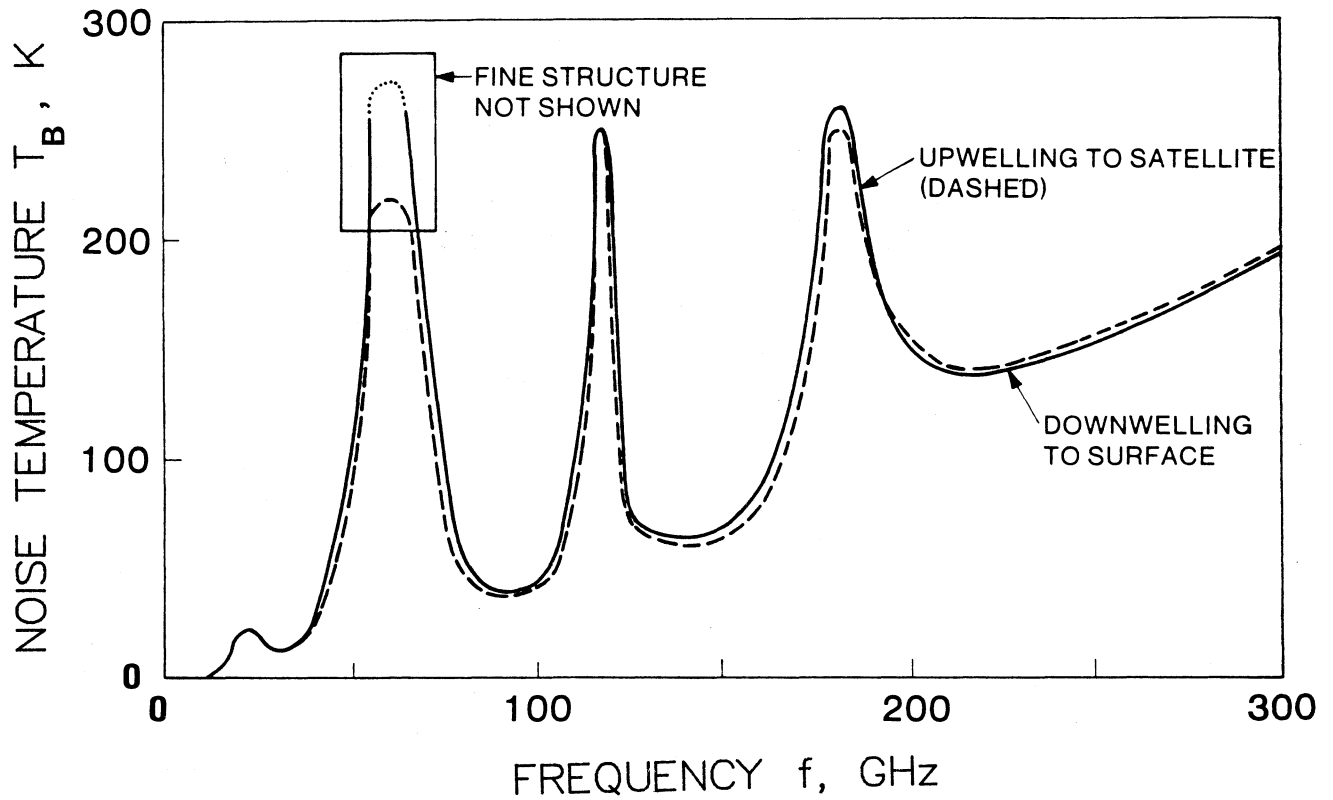
Figure 5.   Atmospheric noise temperatures T_B for upwelling (no surface contribution) and downwelling (no 2.7 deg K cosmic background contribution) radiation along a vertical path through a mid-latitude winter atmosphere (Valley, 1976).

Weighting Function at 58.8 GHz
(Elevation Angle:0,40,90 deg)
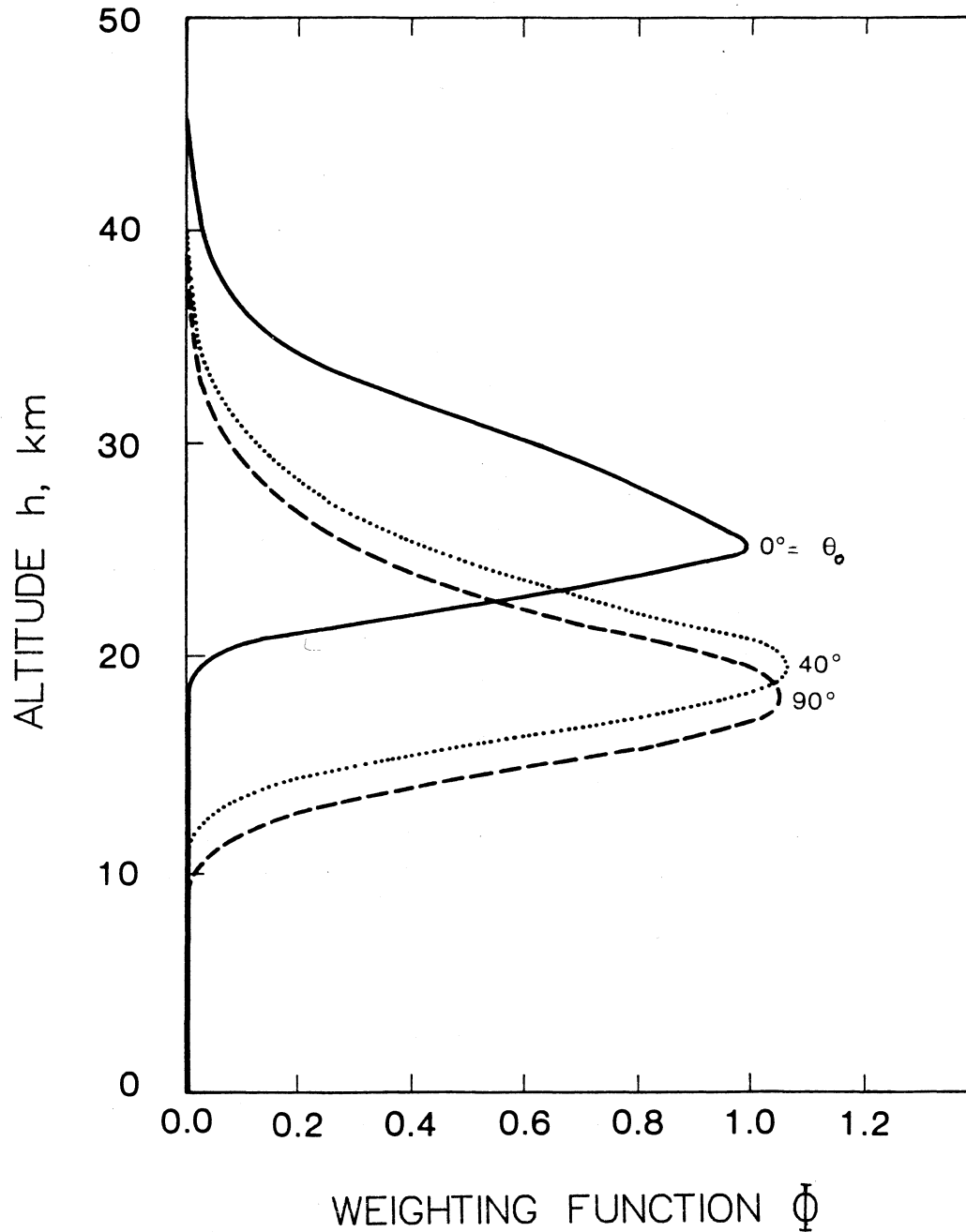
Figure 6.   Weighting functions ϕ_u at 58.82 GHz for three elevations angles θ_0 (at $h_0 = 0$). The model atmosphere is midlatitude winter.

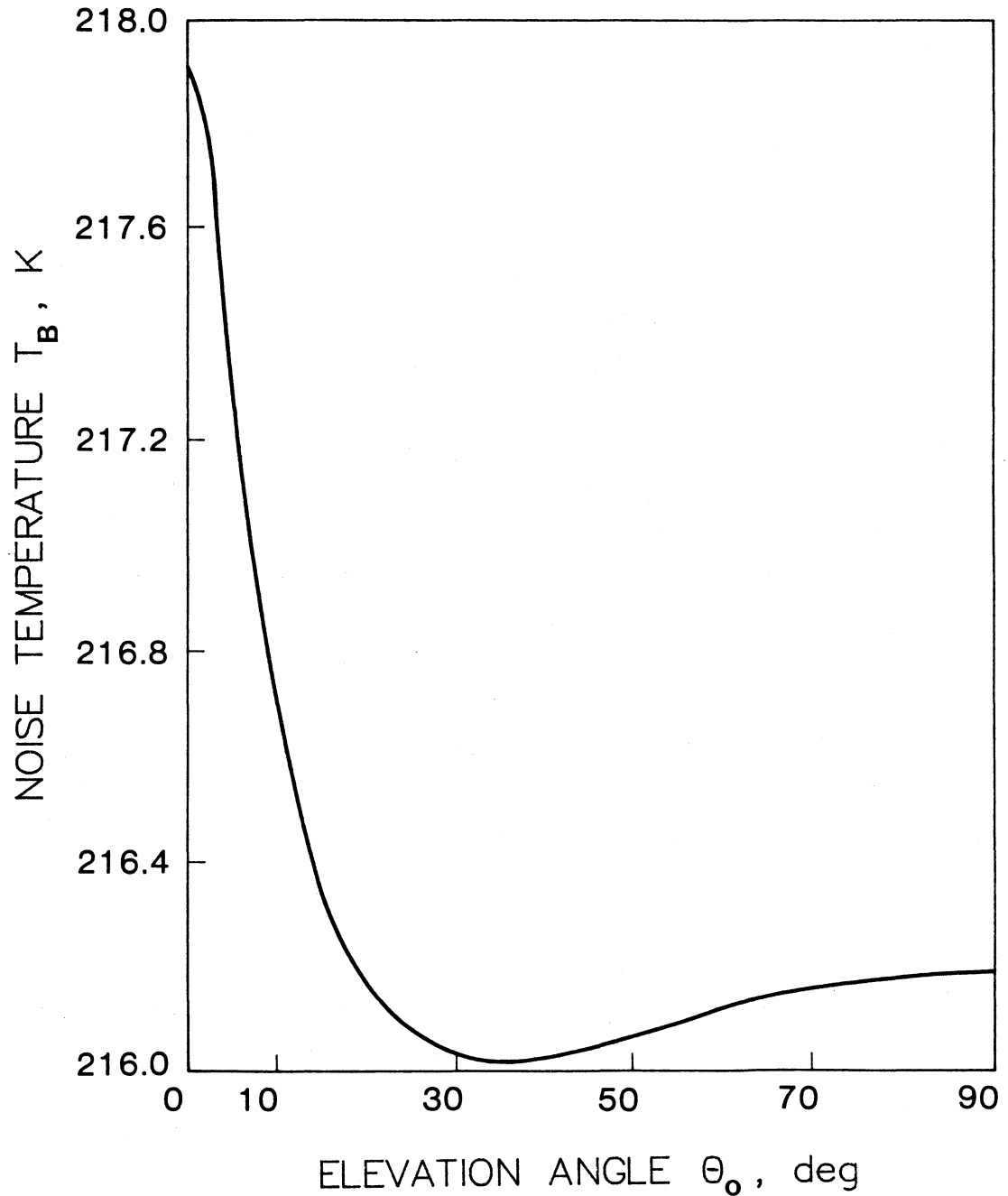# Upwelling Radiance at 58.8 GHz
(Elevation Angle Dependence)

Figure 7.   Upwelling atmospheric noise temperature T_B at 58.82 GHz leaving the atmosphere at H = 80 km for rays that originate at h = 0 km under various angles θ = 0 to 90° (model atmosphere, see Figure 6).

$$T_B^\uparrow = \sum_{i=0}^{m} \tau_u(h_{i+1}, H) \int_{h_i}^{h_{i+1}} \tau_u(h, h_{i+1}) \alpha T dx \qquad\qquad K \qquad (13a)$$

and

$$T_B^\downarrow = \sum_{i=1}^{n} \tau_d(h_o, h_i) \int_{h_i}^{h_{i+1}} \tau_d(h_i, h) \alpha T dx \qquad\qquad K. \qquad (13b)$$

In the expression for the upwelling temperature, the index m is such that $h_{m+1} = H$; while for the downwelling case, n is such that h_{n+1} is a suitable replacement for the infinite limit of integration which appears in (11b). This is not only convenient but also physically meaningful since above approximately 80 km, the absorption is nearly nonexistent (Liebe, 1983) and the assumption of thermodynamic equilibrium begins to break down (Smith, 1982).

Although the summands in the equations for upwelling and downwelling noise temperature can be calculated and summed by the ray tracing program, a pair of recursion relations that actually yield noise temperatures at not only h_o and H, but also at all other heights h_i, are preferable to direct summation. For noise temperature due to radiation flowing along a ray up to height h_{k+1}, it follows that

$$T_B^\uparrow(h_{k+1}) = \int_{h_k}^{h_{k+1}} \tau_u(h, h_{k+1}) \alpha T dx + T_B^\uparrow(h_k) \tau_u(h_k, h_{k+1}) \qquad K. \qquad (14a)$$

Similarly, for downwelling radiation

$$T_B^\downarrow(h_k) = \int_{h_k}^{h_{k+1}} \tau_d(h_k, h) \alpha T dx + T_B^\downarrow(h_{k+1}) \tau_d(h_k, h_{k+1}) \qquad K. \qquad (14b)$$

Heuristically, the recursion relations show that the noise temperature at one side of a layer is the sum of the emission of that layer plus the noise temperature at the opposite side diminished by a transmission factor.

In view of these equations, it is sufficient, in the course of a surface-to-space ray trace, to compute and store the quantities

$$\tau_u(h_k, h_{k+1}), \qquad \int_{h_k}^{h_{k+1}} \tau_u(h, h_{k+1}) \alpha T dx, \text{ and } \qquad \int_{h_k}^{h_{k+1}} \tau_d(h_k, h) \alpha T dx$$

and afterwards to combine them as indicated above.

18

If the temperature T_i at the altitude h_i is perturbed [when, for example, it is required to obtain the Jacobian matrix of partial derivatives in the Backus-Gilbert inversion method (Westwater and Strand, 1974)], only those integrals with h_i as an upper or lower limit need be recomputed, and the recursion relation then applied.

The calculation of total attenuation across a layer is direct. The noise temperature integrals across a layer may, in principle, be evaluated by the adaptive Romberg subroutine (Bauer, 1961) which will require values of the integrands

$$\tau_u(h,h_{k+1})\alpha(h)T(h) \quad \text{and} \quad \tau_d(h_k,h)\alpha(h)T(h)$$

at a number of intermediate heights between h_k and h_{k+1}. The exact number of intermediate heights is determined as a function of the convergence criterion in the adaptive Romberg integration routine.

Since the evaluation of each integrand involves the computation of attenuation across a sublayer of the original layer, such a computation is, in a sense, redundant. Furthermore, computing time increases (and so does expense) as the number of calls to the integration routine increase. Finally, the exponential factors in the noise integrands are nearly the same, except that one goes from the top of the layer downward, while the other goes from the bottom up, thereby introducing yet another apparent redundancy. Therefore, in the interest of more efficient computation, several numerical methods have been devised.

It is first noted that if the temperature T is constant between two successive heights, a and b (which may lie between h_k and h_{k+1}) then

$$\int_a^b \tau_u(h,b)\alpha T dx = T[1 - \tau(a,b)] = \int_a^b \tau_d(a,h)\alpha T dx. \qquad (15)$$

This equation provides a simple means of evaluating the noise integrals across an isothermal layer, as is often postulated or measured in the upper air mass. When the temperature between h_k and h_{k+1} is not constant, the layer may be subdivided into small subintervals such that the temperature over each is

nearly constant. In that case, the noise integrals across the layer are approximated as

$$\int_{h_k}^{h_{k+1}} \tau_u(h,h_{k+1})\alpha T dx \doteq \sum_{i=0}^{L} \tau_u(a_{i+1},h_{k+1})T_i[1 - \tau_u(a_i,a_{i+1})] \quad (16a)$$

and

$$\int_{h_k}^{h_{k+1}} \tau_d(h_k,h)\alpha T dx \doteq \sum_{i=0}^{L} \tau_d(h_k,a_i)T_i[1 - \tau_d(a_i,a_{i+1})]. \quad (16b)$$

Here the points $a_0 = h_k < a_1 < a_2 \ldots < a_{L+1} = h_{k=1}$ define the subintervals of the layer between h_k and $h_{k=1}$ and the number of points a_i is chosen so that the temperature is nearly constant between a_i and a_{i+1} for all $i = 0, 1, \ldots L$. Each summand is readily computed once the intergrals

$$\int_{a_i}^{a_{i+1}} \alpha \, dx, \qquad i = 0, 1, 2, \ldots L$$

are available. Although these may be calculated by calling the integration subroutine, a more efficient approach can be devised.

Between heights h_k and h_{k+1} a curved ray path has the length

$$P = \int_{h_k}^{h_{k+1}} dx, \quad (17)$$

where $dx = s(\Delta h)$ is the differential path length (7b). If the layer is partitioned into $L + 1$ subintervals, as above, then a differential of path length across the interval from a_i to a_{i+1} is approximately

$$dP = \frac{P}{L+1}, \quad (18)$$

and if there is no ray bending then each subsegment has length equal to dP.

When the elevation angle θ is assumed constant and the attenuation varies slowly between h_k and h_{k+1} then $dx = dh/\sin\theta$ and

$$\int_{a_i}^{a_{i+1}} \alpha(h)dx = \frac{\alpha(a_{i+1}) + \alpha(a_i)}{2} \frac{a_{i+1} - a_i}{\sin \theta} = \frac{\alpha(a_{i+1}) + \alpha(a_i)}{2} \int_{a_i}^{a_{i+1}} dx.$$

Let α_i denote the average value of $\alpha(h)$ between a_i and a_{i+1}, so that, if θ is constant, it follows from the definition of dP that

$$\int_{a_i}^{a_{i+1}} \alpha dx = \alpha_i dP$$

and if θ is not constant then this is an approximation. Consequently, the difference

$$\Delta = \int_{h_k}^{h_{k+1}} \alpha dx - \sum_{i=0}^{L} \alpha_i dP$$

may not equal zero. To retain the simplicity of the summation, a correction term for the attenuation values is defined as

$$\delta = \frac{\Delta}{(L+1) \ dP} \ .$$

Then

$$\int_{h_k}^{h_{k+1}} \alpha \ dx - \sum_{i=0}^{L} (\alpha_i + \delta)dP = \Delta - \sum_{i=0}^{L} \frac{\Delta}{(L+1)dP}dP = 0$$

as desired.

5. CONCLUSIONS

Computer simulation of propagation effects is essential to the design of systems operating through the atmosphere. Molecular absorption varies across the 1 to 300 GHz band and poses constraints for transmission and shielding applications. Transfer properties are strongly dependent upon radio path length and elevation angle and also on meteorological conditions. Methods have been presented to model these properties based on physical principles, algorithm stability and efficiency, and computing philosophy. The noise temperature algorithms not only afford a means of obtaining noise temperatures at many points along a ray (only at the expense of the time required to print the additional information) but also provide an elementary method for obtaining the elements of the Jacobian matrix used in temperature inversion. The major limitations of the model result from the great variability of the atmosphere and the sporadic occurrence of clouds and rain, which were not addressed.

6. ACKNOWLEDGMENTS

6. REFERENCES

Bauer, F.L. (1961), La Methode d'Integration Numerique de Romberg, Colloque sur L'Analyse Numerique, held at Mons, France, on March 22-24, pp. 119-129.

Bean, B.R. and G.D. Thayer (1959), CRPL Exponential Reference Atmosphere, National Bureau of Standards Monograph 4 (U.S. Government Printing Office, Washington, D.C.

Blake, L.V. (1968), Ray height computations for a continuous nonlinear refractive index profile, Radio Sci. $\underline{3}$, No. 1, pp. 85-95.

Chandrasekar, S. (1950), Radiative Transfer (Oxford University Press, London).

Levine, D., J. Cromack, and T. Bjorn (1973), Increase of error in range correction with elapsed time, evaluated by ray tracing through radiosonde-generated atmospheric models, Radio Sci. $\underline{8}$, No. 7, pp. 633-639.

Liebe, H.J. (1983), An atmospheric millimeter wave propagation model, NTIA Report 83-137, December, (NTIS Order No. PB84-143494).

Liebe, H.J. (1985), An updated model for millimeter wave propagation in moist air, Radio Sci. $\underline{20}$, No. 5, pp. 1069-1089.

Liebe, H.J., G.G. Gimmestad, and J.D. Hoppenen (1977), Atmospheric oxygen microwave spectrum experiment versus theory, IEEE Trans. Ant. Prop. $\underline{AP-25}$, No. 3, pp. 336-345.

List, R. Jr. (1958), Smithsonian Meteorological Tables, Sixth revised edition, Smithsonian Institution, Washington, D.C.

Rosenkranz, P.W. (1975), Shape of the 5 mm oxygen band in the atmosphere, IEEE Trans. Ant. Prop. $\underline{AP-23}$, No. 4, pp. 498-506.

Smith, E.K. (1982), Centimeter and millimeter wave attenuation and brightness temperature due to atmospheric oxygen and water vapor, Radio Sci. $\underline{17}$, No. 6, pp. 1455-1464.

Smith, E.W. (1981), Absorption and dispersion in the O_2 microwave spectrum at atmospheric pressures, J. Chemical Phys. $\underline{74}$, No. 12, pp. 6658-6673.

Valley, S.L., editor (1976), Handbook of Geophysics and Space Environments (McGraw-Hill Book Corp., New York, New York).

Westwater, E.R. and O.N. Strand (1974), A generalized inversion program, NOAA Technical Report, ERL 309-WPL, Boulder, CO.

BIBLIOGRAPHIC DATA SHEET

1. PUBLICATION NO. NTIA Report 86-204	2. Gov't Accession No.	3. Recipient's Accession No.

4. TITLE AND SUBTITLE A Computational Model for the Simulation of Millimeter-Wave Propagation through the Clear Atmosphere	5. Publication Date October 1986
	6. Performing Organization Code NTIA/ITS.S3

7. AUTHOR(S) Hans J. Liebe & Jerry D. Hopponen	9. Project/Task/Work Unit No. 910 8108
8. PERFORMING ORGANIZATION NAME AND ADDRESS National Telecommunications & Information Administration Institute for Telecommunications Sciences 325 Broadway Boulder, CO 80303 3328	
	10. Contract/Grant No.

11. Sponsoring Organization Name and Address National Telecommunications & Information Administration Herbert C. Hoover Building Washington, D.C. 20504	12. Type of Report and Period Covered
	13.

14. SUPPLEMENTARY NOTES

15. ABSTRACT *(A 200-word or less factual summary of most significant information. If document includes a significant bibliography or literature survey, mention it here.)*

Prediction of propagation effects (i.e., path attenuation, phase delay, ray bending, and medium noise) over the 1 to 300 GHz frequency range through the clear, nonturbulent atmosphere is accomplished by combining a spectroscopic data base with a computer program for two-dimensional ray tracing. Interactions between the physical environment and electromagnetic radiation are expressed by a complex refractivity, N. The quantity N is a function of frequency, pressure, humidity, and temperature. Spectroscopic data supporting N consist of more than 450 coefficients describing local O_2 and H_2O absorption lines complemented by continuum spectra for dry air and water vapor. Height profiles (up to 80 km) of N-spectra are the basis for calculating propagation effects along a radio path (ground-to-ground, ground-to-aircraft, ground-to-satellite). The computer model assumes a symmetric, spherically stratified atmosphere without horizontal N gradients. Evaluation of path integrals for radio range cumulative attenuation, and noise temperature is accomplished in a rapid manner. Various simulated propagation aspects are presented and details of the treatment of the noise integrals are given.

16. Key Words *(Alphabetical order, separated by semicolons)*

clear atmosphere; millimeter-wave propagation; path attenuation and delay; radiances; radio path modeling; ray bending

17. AVAILABILITY STATEMENT ☒ UNLIMITED. ☐ FOR OFFICIAL DISTRIBUTION.	18. Security Class. *(This report)* Unclassified	20. Number of pages 32
	19. Security Class. *(This page)* Unclassified	21. Price: